To be presented at the Fourth Oaxtepec Symposium in
Nuclear Physics, Oaxtepec, Mexico, January 1981.

Master

ANGULAR DISTRIBUTIONS OF SEQUENTIALLY EMITTED PARTICLES AND GAMMA RAYS IN DEEP INELASTIC PROCESSES*

L. G. Moretto

Lawrence Berkeley Laboratory
Nuclear Science Division
University of California
Berkeley, California 94720

Abstract

A general theory for the angular distribution of sequentially emitted particles and gamma rays is developed. Comparison with experimental data allows one to obtain information on the fragment spin and misalignment. Angular distributions of sequentially emitted gamma, alpha and fission fragments are discussed in detail. It is shown that the experimental data are consistent with the thermal excitation of angular momentum bearing modes. The anomaly of sequential fission suggests the presence of a prompt or direct fission component.

DISCLAIMER

DISTRIBUTION OF THIS DOCUMENT IS UNLIMITED

*This work was supported by the Nuclear Science Division of the U. S. Department of Energy under contract No. W-7405-ENG-48.

The figures were printed from originals provided by the author.

Introduction

The interaction between two colliding nuclei leads to the transfer of orbital angular momentum into fragment spin. This phenomenon and its Q value dependence are well documented in the literature of heavy ion reactions.[1-4] A simple model of two colliding spheres leads to the expectation that the fragment spin be aligned with the entrance channel orbital angular momentum, perpendicular to the reaction plane. This is approximately verified experimentally by the anisotropic emission of gamma rays,[5-7] light particles[8] or fission fragments from the primary products.[9-11] However, a more careful observation of the experimental data leads to the conclusion that the fragment spins are not completely aligned, and that the degree of misalignment presents a distinct Q-value dependence.

One may wonder what may be the cause of the spin misalignment. On one hand there is the possibility that the misalignment arises from poorly understood dynamical effects like (induced) multipole-(induced) multipole interactions through the nuclear and/or Coulomb field.

On the other hand, statistical effects may come into play. The dinuclear complex is characterized by angular-momentum-bearing modes whose thermal excitation may introduce in-plane angular momentum components which misalign the fragment spin.[12] The coupling responsible for the thermal excitation of these modes may still be the multipole-multipole interaction. The advantage of the equilibrium statistical limit is that we do not have to bother to describe it in any detail.

In view of this advantage we shall consider the prediction of the equilibrium statistical limit. We shall then apply this result to the sequential γ-ray emission and we shall compare with the data. Similarly we shall apply the result of the statistical model to the sequential alpha particle emission and to sequential fission. Again we shall compare with the data. In the end we shall show some intriguing anomaly in sequential fission that seems to indicate the presence of prompt or direct sequential fission in contrast with the commonly held view that sequential fission arises from compound nucleus decay of a deep inelastic fragment.

Statistical Excitation of Angular-Momentum-Bearing Modes

Let us consider a frame of reference where the z axis is parallel to the entrance-channel angular momentum, the x axis is parallel to the recoil direction of one of the fragments, and the y axis is perpendicular to the z,x plane.

If the intermediate complex is assumed to have the shape of two equal touching spheres, the angular-momentum-bearing normal modes are easily identifiable. In fig. 1 these modes are illustrated. We shall call them "bending," B (doubly degenerate), "twisting" Tw (degenerate with bending), "wriggling" W (doubly degenerate) and "tilting" Ti.

In a recent work, the statistical mechanical aspects of the excitation of these modes has been studied in detail.[12] Here we report only the relevant conclusions.

The thermal excitation of these collective modes leads to Gaussian distributions in the three components I_x, I_y, I_z, namely:

$$P(\underline{I}) \quad \exp - \left(\frac{I_x^2}{2\sigma_x^2} + \frac{I_y^2}{2\sigma_y^2} + \frac{(I_z - \bar{I}_z)^2}{2\sigma_z^2} \right) \tag{1}$$

where:

$$\sigma_x^2 = \sigma_{Tw}^2 + \sigma_{Ti}^2 = \frac{1}{2}\mathcal{J}T + \frac{7}{10}\mathcal{J}T = \frac{6}{5}\mathcal{J}T$$

$$\sigma_y^2 = \sigma_B^2 + \sigma_w^2 = \frac{1}{2}\mathcal{J}T + \frac{5}{14}\mathcal{J}T = \frac{6}{7}\mathcal{J}T \tag{2}$$

$$\sigma_z^2 = \sigma_B^2 + \sigma_w^2 = \frac{1}{2}\mathcal{J}T + \frac{5}{14}\mathcal{J}T = \frac{6}{7}\mathcal{J}T \quad .$$

The quantity $\mathcal{J}$ is the moment of inertia of one of the two touching spheres, and T is the temperature.

Notice that the variances along the three coordinates are almost equal.

Frequently the degree of alignment of the fragment spins is expressed in terms of the alignment parameter $P_{zz} = 3/2\ \bar{I}_z^2/\bar{I}^2 - 1/2$. If $\sigma_x = \sigma_y = \sigma_z = \sigma$ it is possible to express the alignment parameter P_{zz} in terms of σ and the average z component of the fragment angular momentum I_z as follows:

$$P_{zz} = \frac{3}{2}\ \frac{\bar{I}_z^2}{\bar{I}^2} - \frac{1}{2} = \frac{3}{2}\ \frac{\bar{I}_z^2 + \sigma^2}{\bar{I}_z^2 + 3\sigma^2} - \frac{1}{2} \quad .$$

Gamma Ray Angular Distributions

Fragments with large amounts of angular momentum are expected to dispose of it mainly by stretched E2 decay. The relative amounts of dipole and quadrupole radiation depend mainly upon the ability of the nucleus to remain a good rotor over the whole angular momentum range.

If the angular momentum of the fragment is aligned, the typical angular pattern of the quadrupole radiation should be observed. Any misalignment should decrease the sharpness of the angular distribution.

If the distribution of the angular momentum components I_x, I_y, I_z is statistical, it is straightforward to derive analytical expressions for the angular distributions.[13]

For a perfectly aligned system we have:

$$W(\alpha) = \frac{3}{4}(1 + \cos^2\alpha) \quad ; \quad W(\alpha) = \frac{5}{4}(1 - \cos^4\alpha)$$

for E1 for E2

If the angular momentum is not aligned with the z axis, one must express α in terms of θ, ϕ which define the direction of the angular momentum vector. In particular we have:

$$\cos\alpha = \frac{\underline{I}\cdot\underline{n}}{I} = \frac{I_x \sin\theta \cos\phi + I_y \sin\theta \sin\phi + I_z \cos\theta}{(I_x^2 + I_y^2 + I_z^2)^{1/2}}$$

For any given I, the angular distribution is obtained by integration over the statistical distribution $P(\underline{I})$ of the angular momentum components:

$$W(\theta,\phi) = \int W(\alpha)\ P(\underline{I})\ d\underline{I}$$

It is not possible to obtain exact analytical expression for the general case. However, an expansion to order $\sigma_x^2/\bar{I}_z^2$, $\sigma_y^2/\bar{I}_z^2$, etc. allows one to obtain expressions in closed form.

For the dipole decay we have:

$$W(\theta,\phi) = \frac{3}{4}(1 + \cos^2\theta) + \frac{3}{4}\left[(\sin^2\theta\ \cos^2\phi - \cos^2\theta)\ \frac{\sigma_x^2}{\bar{I}_z^2} + (\sin^2\theta\ \sin^2\phi - \cos^2\theta)\ \frac{\sigma_y^2}{\bar{I}_z^2}\right] \tag{3}$$

Notice that there is no dependence upon σ_z^2. A weak in-plane anisotropy is possible:

$$\frac{W(\phi = 0^\circ)}{W(\phi = 90^\circ)}_{\theta=90^\circ} = \frac{1 + \sigma_x^2/\bar{I}_z^2}{1 + \sigma_y^2/\bar{I}_z^2} \cong 1 + \frac{\sigma_x^2 - \sigma_y^2}{\bar{I}_z^2} \tag{4}$$

The out-of-plane anisotropy for equal values of σ_x, σ_y, σ_z, is

$$\frac{W(0^\circ)}{W(90^\circ)} = 2\ \frac{(1 - \sigma^2/\bar{I}_z^2)}{(1 + \sigma^2/\bar{I}_z^2)} \simeq 2(1 - 2\sigma^2/\bar{I}_z^2) \tag{5}$$

For the quadrupole decay we have:

$$W(\theta,\phi) = \frac{5}{4}(1 - \cos^4\theta) - \frac{5}{2}\left[(3\sin^2\theta\cos^2\theta\cos^2\phi - \cos^4\theta)\frac{\sigma_x^2}{\bar{I}_z^2}\right.$$

$$\left. + (3\sin^2\theta\cos^2\theta\sin^2\phi - \cos^4\theta)\frac{\sigma_y^2}{\bar{I}_z^2}\right] \qquad (6)$$

Again, no dependence upon σ_z^2 is predicted. Assuming σ_x, $\sigma_y = \sigma_z = \sigma$ one obtains

$$\frac{W(0^\circ)}{W(90^\circ)} \simeq 4\frac{\sigma^2}{\bar{I}_z^2} \qquad (7)$$

For the in plane anisotropy we have:

$$\left.\frac{W(\phi = 0^\circ)}{W(\phi = 90^\circ)}\right|_{\theta=90^\circ} \sim 1 \qquad (8)$$

to order $\sigma^2/\bar{I}_z^2$. This can be easily understood. The rms misalignment is $\sim\sigma/I$, thus, at $\theta = 90^\circ$:

$$W(90) = 1 - \cos^4 90^\circ - \frac{\sigma}{I} \simeq 1 - \frac{\sigma^4}{I^4}$$

Thus, no second order term exists. <u>This result shows that its is very difficult to study anisotropies in the angular momentum misalignment by means of γ-ray angular distribution.</u>

The range of validity of the above expressions is rather limited due to the low order expansion. In particular, the equations should not be trusted for $\sigma^2/\bar{I}_z^2 > 0.05$.

However, if we are willing to assume $\sigma_x^2 = \sigma_y^2 = \sigma_z^2 = \sigma$ then an exact result can be obtained.

For the E1 distribution one obtains:

$$W(\theta)_{E1} = \frac{3}{4}\left[1 + \cos^2\theta + \lambda^2(1 - D(\lambda))(1 - 3\cos^2\theta)\right] \tag{9}$$

For the E2 distribution one obtains:

$$\begin{aligned} W(\theta)_{E2} = \frac{5}{4}\Big[1 &- \cos^4\theta - 2\lambda^2\Big\{3\sin^2\theta\cos^2\theta - 2\cos^4\theta + \\ &- \frac{3}{4}D(\lambda)(\sin^2\theta - 4\cos^2\theta)\sin^2\theta\Big\} + \\ &- 3\lambda^4\Big\{4\cos^4\theta + \frac{3}{2}\sin^4\theta - 12\sin^2\theta\cos^2\theta\Big\}(1 - D(\lambda))\Big] \end{aligned} \tag{10}$$

In these equations $\lambda = \sigma/\bar{I}_z$ and $D(\lambda) = \sqrt{2}\,\lambda\, F(1/\sqrt{2}\,\lambda)$ where

$$F(x) = e^{-x^2}\int_0^x e^{t^2}dt$$

is the Dawson's integral. One can verify immediately that both expressions behave as expected in the limits of $\lambda = 0$ and $\lambda = \infty$. The anisotropy $W(0)/W(90^\circ)$ tends to 1 when λ tends to infinity both for E1 and E2 transitions, while it tends to 0 for E2 and to 2 for E1 when $\lambda = 0$.

These results are graphically summarized in fig. 2 where the anisotropy is plotted as a function of the fraction of E1 radiation for various values of $\sigma^2/\bar{I}_z^2$. The two extreme possibilities of stretched and non-stretched E1 decay are considered.

Application to Experimental γ-Ray Angular Distributions

An interesting measurement has been carried out for the reaction[7] 1400 MeV ^{165}Ho + ^{165}Ho. This system was chosen because large amounts of angular momentum can be transferred into the intrinsic spin of these nuclei, which are known to have good rotational properties. As a consequence, both of the essentially identical DI-fragments emit similar continuum γ-ray spectra which are strongly enriched in E2 transitions (~80 percent).

Figure 3 (top) shows the dependence of the γ-ray multiplicity upon Q-value for three angles. Figure 3 (middle) shows the intrinsic spin of one of the two reaction fragments after neutron emission (solid line). The primary fragment spin obtained from $\langle M_\gamma \rangle$ with correction for neutron emission (dashed line) is also shown.

The ratio of in-plane to out-of-plane γ-ray yield ("anisotropy") for energies between 0.6 and 1.2 MeV is also shown in fig. 3 (bottom). This anisotropy rises with increasing spin transfer; it peaks at a value of ~2.2, slightly before the spin saturates, and then drops to near unity for large Q-values.

The initial rise of anisotropy with increasing Q-value indicates that during the early stages of energy damping there is a rapid buildup of aligned spin. The subsequent fall observed at larger Q-values

suggests that the aligned component of spin has saturated or is decreasing, whereas randomly-oriented components continue to increase, causing a significant decrease in the alignment of the fragments' spin.

Figure 4 shows experimental values of the anisotropy for E_γ greater than 0.6 MeV compared to several stages of the model calculation. The spin $\langle I \rangle$ was determined from the γ-ray multiplicity, and the anisotropy was then calculated (solid line). This calculation reproduces both the shape and the magnitude of the data. To give a feeling for the importance of various contributions, the same calculation is shown including only E1 transitions (dashed curve) and including E1 transitions and neutron emission (dotted line). The hatching on the solid curve indicates the uncertainty of the overall calculation. This comparison clearly shows that the most important effect is the thermally induced misalignment, indicating that the decrease of alignment as deduced from the anisotropy is inherent to the deep-inelastic process itself.

The dependence of the alignment parameter and of the z component of angular momentum is shown in fig. 5.

A provisional conclusion is that the equilibrium statistical limit is very close to the regime controlling the spin misalignment in this reaction.

Angular Distributions of Sequential Fission and of Sequential Light Particle Emission

The magnitude of the angular momentum misalignment can be measured through the in- and out-of-plane angular distribution of the decay product of one of the two fragments. It has been shown elsewhere that

the angular distribution of fission fragments and of light particles emitted by a compound nucleus can be treated within a single framework.[14]

The direction of emission of a decay product (fission fragment, α-particle, etc) is defined by the projection K of the fragment angular momentum on the disintegration axis. Simple statistical mechanical considerations show that the distribution in K values is Gaussian.

Specifically, for any given K, the particle decay width can be written as:[13,14]

$$\Gamma_K^I \, dK = \Gamma^{\bullet} \exp\left[-\frac{\hbar^2 I^2}{2T}\left(\frac{1}{\mathcal{J}_\perp} - \frac{1}{\mathcal{J}_c}\right)\right] \exp\left(-\frac{K^2}{2K_0^2}\right)\frac{dK}{T} \tag{11}$$

where $\Gamma^{\bullet}$ is an angular momentum independent quantity; T is the temperature; $K_0^2 = \hbar^{-2}(1/\mathcal{J}_\parallel - 1/\mathcal{J}_\perp)^{-1}T$; $\mathcal{J}_\parallel$, $\mathcal{J}_\perp$ are the principal moments of inertia of the decaying system with particle and residual nucleus just in contact, about an axis parallel and perpendicular to the disintegration axis respectively; $\mathcal{J}_c$ is the moment of inertia of the compound nucleus.

Similarly, the neutron decay width, integrated over all the neutron emission directions is

$$\Gamma_N = \Gamma_N^{\bullet} \exp\left[-\frac{\hbar^2 I^2}{2T}\left(\frac{1}{\mathcal{J}_N} - \frac{1}{\mathcal{J}_c}\right)\right] \tag{12}$$

In this expression $\mathcal{J}_N = \mathcal{J}_R + \mu R^2$, corresponding to $\mathcal{J}_\perp$ in eq. (3), is the sum of the moment of inertia of the residual nucleus after

neutron decay and the orbital moment of inertia of the neutron at the surface of the nucleus.

Let us now express the particle decay width in terms of the emission angle α measured with respect to the angular momentum direction.

Since $K = I \cos\alpha$ and $dK = Id(\cos\alpha) = Id\Omega$, we obtain:

$$\Gamma^{I}(\alpha)\, d\Omega = \Gamma^{0} \exp\left[-\frac{\hbar^2 I^2}{2T}\left(\frac{1}{\mathcal{J}_1} - \frac{1}{\mathcal{J}_c}\right)\right] \exp - \frac{I^2\cos^2\alpha}{2K_0^2}\, d\Omega$$

If the angular momentum has an arbitrary orientation with respect to our chosen frame of reference, defined by its components I_x, I_y, I_z, the angular distribution can be easily rewritten by noticing that

$$K = I\cos\alpha = \underline{I}\cdot\underline{n} = I_x \sin\theta \cos\phi + I_y \sin\theta \sin\phi + I_z \cos\theta$$

where $\underline{n}$ is a unit vector pointing the direction of particle emission with polar angles θ,ϕ. Integration over the distribution $P(\underline{I})$ leads to the following expression, dropping angular momentum independent factors:[13,15]

$$\Gamma^{I}(\theta,\phi)\, d\Omega \propto \exp\left[-\frac{\hbar^2 I^2}{2T}\left(\frac{1}{\mathcal{J}_1} - \frac{1}{\mathcal{J}_c}\right)\right] \frac{1}{S(\theta,\phi)} \exp - \frac{I^2\cos^2\theta}{2S^2(\theta,\phi)}\, d\Omega \qquad (13)$$

where:

$$S^2(\theta,\phi) = K_0^2 + (\sigma_x^2 \cos^2\phi + \sigma_y^2 \sin^2\phi) \sin^2\theta + \sigma_z^2 \cos^2\theta \tag{14}$$

The final angular distribution is obtained by integration over the fragment angular momentum distribution which we assume to reflect the entrance channel angular momentum distribution through the rigid rotation condition:

$$W(\theta,\phi) \propto \int_{I_{min}}^{I_{mx}} \frac{2I}{S} \exp -\left(I^2 \frac{\cos^2\theta}{2S^2} - \beta\right) dI \tag{15}$$

where we have made the frequently valid approximation $\Gamma_T \approx \Gamma_N$ or more explicitly

$$W(\theta,\phi) = \frac{1}{S}\left[\frac{I_{min}^2}{A_{min}} \exp(-A_{min}) - \frac{I_{min}^2}{A_{mx}} \exp(-A_{mx})\right] \tag{16}$$

where

$$A_{mx} = I_{mx}^2\left[\frac{\cos^2\theta}{2S^2} - \beta\right] \; ; \quad A_{min} = I_{min}^2\left[\frac{\cos^2\theta}{2S^2} - \beta\right] \tag{17}$$

$$\beta = \frac{\hbar^2}{2T}\left(\frac{1}{\mathcal{J}_n} - \frac{1}{\mathcal{J}_\perp}\right)$$

The quantity $\mathcal{J}_n$ is the moment of inertia of the nucleus after neutron emission, $\mathcal{J}_\perp$ is the perpendicular moment of inertia of the critical shape for the decay (e.g., saddle point).[14]

It is important to notice that the angular momentum dependence of the particle/neutron competition or fission/neutron competition is explicitly taken into account through β.

The final ingredient necessary for an explicit calculation of the angular distributions is the quantity K_0^2. This quantity can be expressed in terms of the principal moments of inertia of the critical configuration for the decay:

$$K_0^2 = \frac{1}{h^2}\left(\frac{1}{\mathcal{J}_{\parallel}} - \frac{1}{\mathcal{J}_{\perp}}\right)^{-1} T = \mathcal{J}_{eff} T \tag{18}$$

For fission $\mathcal{J}_{eff}$ can be taken from the liquid drop calculations.[16] For lighter particle emission, the calculation of $\mathcal{J}_{eff}$ can be worked out trivially.

If the charge of the light particle is not negligible, one has to consider the shape polarization induced on the heavy fragment at the ridge point, as discussed in ref. 14.

Now we are in the position to calculate both in-plane and out-of-plane anisotropies.

The in plane anisotropy gives:

$$\left.\frac{W(\phi = 90^\circ)}{W(\phi = 0^\circ)}\right|_{\theta=90^\circ} = \left(\frac{K_0^2 + \sigma_x^2}{K_0^2 + \sigma_y^2}\right)^{1/2} \tag{19}$$

Since in most cases K_0^2 is fairly large, or at least comparable with σ_x^2 or σ_y^2, it is difficult to obtain a sizable in-plane anisotropy.

Even by letting $\sigma_x = 0$ one needs $\sigma_y^2 = 3\,K_0^2$ just to obtain the anisotropy of 2! The out-of-plane anisotropy is somewhat more complicated: For a fixed angular momentum I one has:

$$\left.\frac{W(\theta = 90^\circ)}{W(\theta = 0^\circ)}\right|_{\phi=0^\circ} = \left(\frac{K_0^2 + \sigma_z^2}{K_0^2 + \sigma_x^2}\right)^{1/2} \exp\left(\frac{I^2}{2(K_0^2 + \sigma_z^2)}\right) \quad . \tag{20}$$

For the usual angular momentum distribution one obtaines:

$$\left.\frac{W(\theta = 90^\circ)}{W(\theta = 0^\circ)}\right|_{\phi=0^\circ} = \frac{1}{\beta}\left(\frac{K_0^2 + \sigma_z^2}{K_0^2 + \sigma_x^2}\right)^{1/2} \left(\beta - \frac{1}{2(K_0^2 + \sigma_z^2)}\right) \tag{21}$$

$$\times \frac{1 - \exp \beta I_{mx}^2}{1 - \exp I_{mx}^2 \left(\beta - \frac{1}{2(K_0^2 + \sigma_z^2)}\right)}$$

At $\phi = 90^\circ$ the anisotropy is obtained from the above equation by interchanging σ_x with σ_y.

Some Calculations for Sequential Fission and Alpha Decay and Comparison with Data

The results obtained above can be illustrated by applying them to a reaction which has been experimentally investigated. We choose the reaction 600 MeV ^{86}Kr + Au.[9] For this reaction we estimate $\mathcal{J}_{sph}/\mathcal{J}_{eff} = 1.864$, $K_0^2 = 100\ \hbar^2$, $\beta = 0.00194\ \hbar^{-2}$, $I_{mx} = 40\hbar$, $\sigma^2 = 110\ \hbar^2$. In order to simultaneously appreciate the shapes of the in- and out-of-plane angular distributions possible in sequential

fission, we have artificially set $\sigma_x^2 = 0$, $\sigma_y^2 = \sigma_z^2 = 110\,\hbar^2$. The results are shown in fig. 6. In this figure one readily observes the connection between the in-plane and the out-of-plane angular distributions. In particular, it is apparent how an in-plane anisotropy must necessarily be associated with a variation of the out-of-plane width with the in-plane angle.

We have stressed already that the competition between fission and neutron decay must be dealt with specifically because of the strong dependence of Γ_F upon angular momentum. This is illustrated in fig. 7 where we have set $\sigma_x^2 = \sigma_y^2 = \sigma_z^2 = 110\,\hbar^2$ and we have assumed $\beta = 0.00194\,\hbar^{-2}$ in one case, and $0.000\,\hbar^{-2}$ in the other. The effect is quite dramatic, and clearly must be incorporated in the formalism if one intends to obtain reliable angular momentum values from it. For instance, in order to compensate for setting $\beta = 0.000$ instead of $0.00194\,\hbar^{-2}$ it is necessary to step-up the angular momentum I_{mx} from 40 to 55 $\hbar$.

The predicted FWHM = 54° can be compared with the data[9] shown in fig. 8. The agreement is quite satisfactory.

In the same spirit as for sequential fission we show some calculations for sequential alpha decay in the reaction 664 MeV ^{84}Kr + Ag. The alpha particles are assumed to be emitted by the Ag-like nucleus. We estimate $I_{mx} = 36\,\hbar$, $\sigma^2 = 68\,\hbar^2$, $\beta = 0.00137\,\hbar^{-2}$ and $K_0^2 = 365\,\hbar^2$. The results are shown in fig. 9. For comparison a calculation with $\sigma^2 = 0$ is also shown in order to illustrate the sensitivity to misalignment. Examples of fits to experimental data[8] are shown in

fig. 10. From these data it is possible to infer the dependence of the heavy fragment spin upon mass asymmetry. It is observed that its value is close to that of rigid rotation (fig. 11).

The Puzzle of the In-Plane Angular Distributions

We have specifically disregarded the in-plane angular distributions in the above discussion of the data. We want to take up the subject here in some detail.

The theory makes specific predictions about the in-plane distribution of both sequential alphas and fission. For symmetric splitting, the model predict $\sigma_y \simeq \sigma_x$ and eq. (19) implies in-plane isotropy. The sequential alphas from Kr + Ag seem to satisfy the theoretical prediction. Sequential fission is another matter. In contrast to previous measurements, the latest results on Ni + Pb and Ar + Bi (ref. 17) show strong in-plane anisotropies peaked along the recoil direction (x-axis). Before accusing the statistical model of gross failure, one should appreciate that the above systems are highly asymmetric and the statistical model ought to take this fact into account. Unfortunately it is very obvious that the introduction of asymmetry in the model worsens the situation. By direct inspection of the normal modes, one realizes that those modes involving the rotation of the two fragments with equal and opposite spin become stiffer with increasing asymmetry because they force a small fragment (small moment of inertia) to rotate with a large spin. This is very expensive in energy. Bending, Twisting and Wriggling modes are part of this category. On the other hand, Tilting clearly becomes softer with

increasing asymmetry, because the difference in the two principal moments of inertia becomes progressively smaller. The inevitable conclusion is that, at large asymmetries, Tilting must dominate, so σ_x grows while σ_y decreases. This does generate strong in-plane anisotropies, but peaked at 90° to the recoil direction! The predicted angular distributions are 90° out-of-phase to the data! An exact calculation shown in fig. 12 indicates that our qualitative predictions for the behavior of σ_x, σ_y and σ_z with asymmetry are quite correct.

In order to make the situation even more extreme we have studied the in-plane sequential fission angular distribution in the reaction and Ne + U (fig. 13). Because of the extreme asymmetry one would expect a strong minimum along the recoil direction and a strong maximum at 90° in plane. Again the experiment is lamentably out of phase with the theory. The in-plane angular distributions are isotropic for the quasi elastic components but peak strongly along the recoil direction for the deep inelastic component.

In view of these data one tends to become very suspicious. If the angular momentum is responsible for the angular distributions, one would expect that the increased stiffness of Bending, Twisting and Wriggling and the decreasing stiffness of Tilting should lead to an angular distribution peaked at 90° to the recoil direction at extreme asymmetries irrespective of whether a dynamical or statistical regime prevails. We can rephrase the same idea by saying that it is expensive if not impossible to load a Ne-like fragment with a large angular

momentum. Tilting is the only normal mode that does not require Ne to do so.

Consequently the suspicion may arise that for sequential fission at least, angular momentum is not totally responsible for the in-plane distribution. The alternative is the following. If the fragment in the exit channel is substantially elongated, as we know it is, it may decide to keep on deforming along the dinuclear axis until it fissions. If this is the case, the fission fragments will tend naturally to peak along the recoil axis. In other words one may invoke prompt fission of the highly deformed fragment rather than compound nucleus fission.

This should be taken as a working hypothesis, but we feel at this time that it ought to be taken seriously. Why then do the α and γ angular distribution behave so much in agreement with the statistical model? The answer is clear. If the deformed fragment in the exit channel is not deformed enough to undergo fission, it may relax into a spherical shape and become a compound nucleus. This compound nucleus then emits α's and γ's and their angular distribution will be of course controlled exclusively by the angular momentum. One cannot rule out the possibility that a sizeable mixture of prompt and compound fission may be present. This clearly requires a larger body of data and a careful analysis.

References

1. R. Reginbart, A. Behkami, G. J. Wozniak, R. P. Schmitt, J. J. Sventek and L. G. Moretto, Phys. Rev. Lett. 41, 1355 (1978).

2. M. M. Aleonard, G. J. Wozniak, P. Glässel, M. M. Deleplanque, R. M. Diamond, L. G. Moretto, R. P. Schmitt and F. S. Stephens, Phys. Rev. Lett. 40, 622 (1978).

3. P. Glässel, ... S. Simon, R. M. Diamond, R. C. Jared, I. Y. Lee, L. G. Moretto, J. O. Newton, R. Schmitt and F. Stephens, Phys. Rev. Lett. 38, 331 (1977).

4. J. B. Natowitz, N. M. Namboodiri, P. Kasiraj, R. Eggers, L. Adler, P. Goutier, C. Cerutti and T. Alleman, Phys. Rev. Lett. 40, 751 (1978).

5. H. Puchta, W. Dunnweber, H. Hering, L. Lauterbach and W. Trautmann, Phys. Rev. Lett. 43, 623 (1979).

6. P. Aguer, G. J. Wozniak, R. P. Schmitt, D. Habs, R. M. Diamond, C. Ellegard, D. Hillis, C. C. Hsu, G. J. Mathews, L. G. Moretto, G. U. Rattazzi, C. P. Roulet, and F. Stephens, Phys. Rev. Lett. 43, 1778 (1979).

7. G. J. Wozniak, R. J. McDonald, A. Pacneco, C. C. Hsu, D. J. Morrissey, L. G. Sobotka, L. G. Moretto, S. Shih, C. Schuck, R. M. Diamond, H. Kluge and F. S. Stephens, Phys. Rev. Lett. 45, 1081 (1980).

8. L. G. Sobotka, G. C. Hsu, G. S. Wozniak, G. U. Rattazzi, R. J. McDonald, A. Pacheco and L. G. Moretto, LBL-11148.

9. G. J. Wozniak, R. P. Schmitt, P. Glässel, R. C. Jared, G. Bizard, and L. G. Moretto, Phys. Rev. Lett. 40, 1436 (1978).

10. P. Dyer, R. J. Puigh, R. Vandenbosch, T. D. Thomas, M. S. Zisman and L. Nunnely, Nucl. Phys. A322, 205 (1979).

11. H. Specht, Lecture Notes in Physics 92, 1, 1979, ed. B. A. Robson.

12. L. G. Moretto and R. P. Schmitt, Phys. Rev. C21, 204 (1980).

13. L. G. Moretto, S. Blau, A. Pacheco, LBL-10805.

14. L. G. Moretto, Nucl. Phys. A247, 211 (1975).

15. R. A. Broglia, G. Pollarolo, C. H. Dasso and T. Dössing, Phys. Rev. Lett. 43, 1649 (1979).

16. S. Cohen, F. Plasil and W. S. Swiatecki, Ann. Phys. 82, 557 (1974).

17. C. LeBrun, J. F. Lecolley, F. Lefevres, M. L'Haridon, A. Osmont, J. P. Patry, J. C. Steckmeyer and R. Chechick, preprint.

Figure Captions

Fig. 1. (a) A pictorial description of the tilting mode and of the doubly degenerate wriggling modes for the two equal sphere model. The arrow originating at the point of tangency represents the orbital angular momentum while the shorter arrows represent the individual fragment spins.
(b) A pictorial illustration of the twisting and bending modes for the two equal sphere model. Note the pairwise cancellation of the fragment spins.

Fig. 2. (a) Gamma-ray anisotropy for a mixture of stretched E1 and E2 transitions as a function of the fraction of E1 radiation for various values of $\sigma^2/\bar{I}_z^2$. (b) Same as in a) but for a mixture of isotropic E1 and stretched E2 transitions.

Fig. 3. Top: Gamma-ray multiplicities vs Q values. The open dots correspond to the 0° measurements, the solid dots correspond to the 90° measurements and the solid line corresponds to the average multiplicity. Middle: The average spin per fragment inferred from the data on the top part of the figure. The solid lines and dashed lines correspond to the spin after and before neutron emission respectively. Bottom: Gamma-ray anisotropies vs Q value.

Fig. 4. Experimental γ-ray anisotropy (E_γ > 0.3 MeV) vs Q-value (open circles). The dashed line represents a calculation including oly the statistical gamma-rays, the dotted line includes neutron emission as well, the solid line includes also the thermal excitation of angular momentum bearing modes. The hatching indicates the range of uncertainty of the calculation.

Fig. 5. a) Dependence of the alignment parameter upon Q-value, as obtained from the calculations illustrated in fig. 4. The dotted line includes only neutron emission, the dashed line includes only the thermal excitation of the angular momentum bearing modes, the solid line includes both effects.
b) Angular momentum before neutron emission (solid line). Angular momentum projection I_z before neutron emission (dashed line). Angular momentum projection I_z after neutron emission (dotted line).

Fig. 6. Calculated in-plane (dashed line) and out-of-plane (solid lines) angular distributions for sequential fission fragments in the reaction 60 MeV Kr + Au. The in-plane anisotropy is artifically generated by setting $\sigma_x = 0$.

Fig. 7. Calculated sequential fission angular distributions for the system 600 MeV Kr + Au. The curve labeled $\beta = 0.0$ corresponds to disregarding neutron emission fission competition. The more realistic curve labeled $\beta = 0.00194$ gives a FWHM of 54°.

Fig. 8. Experimental full width at half maximum of the out-of-plane angular distribution for fission and non-fission components as a function of Z in the reaction 618 MeV ^{86}Kr + ^{197}Au.[9] The squares represent the data in the lab system, the triangles the data in the center of mass of the Au-like fragment. The dots represent the non fissioning Au-like recoils.

Fig. 9. Calculated out-of-plane angular distribution for sequential alpha decay from the Ag-like fragment in the reaction 664 MeV ^{84}Kr + ^{nat}Ag (dashed line).[7] The solid line has been obtained by setting $\sigma = 0$.

Fig. 10. Experimental alpha particle angular distributions for several Z-bins as a function of out-of-plane angle for the same reaction as in Fig. 9. The Z bins are 3 Z's wide and are indicated by the median Z. In Section (a) there is no coincident γ-ray requirements while in (b) there are 2 or more coincident γ-rays. The curves in section (b) are normalized at 90° to those in (a) for the same Z bin.

Fig. 11. Average heavy fragment spin as a function of the light fragment atomic number. The dots represent the spins extracted from data without γ-ray coincidence requirement. The open circles represent the spins obtained when 2 or more γ-rays are required in coincidence. The line represents the rigid rotation limit for two equally deformed spheroids with ratio of axis 2:1.[7]

Fig. 12. a) Variance of the light fragment spin associated with the various normal modes are a function of mass asymmetry. The variance is measured in natural units. $\mathcal{J}_0 T$ is the product of the moment of inertia of one of the two equal spheres and the temperature. b) Same as in a) for the heavy fragment.

Fig. 13. In- and out-of-plane angular distribution for the reaction ^{238}U + Ne. The top points correspond to a Q-value range 0,-50 MeV, the intermediate points to a Q-value range -50,-100 MeV, the bottom points to a Q-value range -100,-200 MeV.

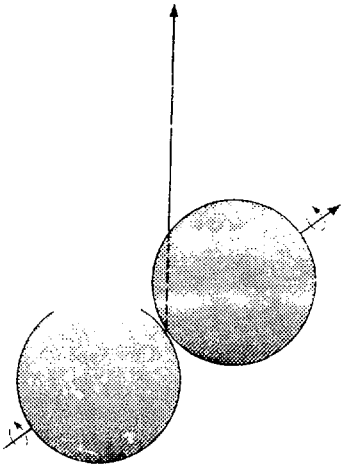

Tilting

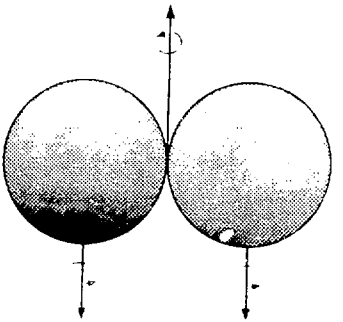

Wriggling

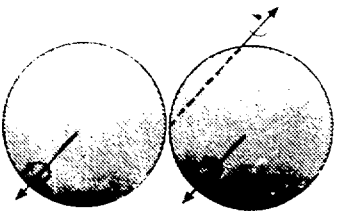

Wriggling

XB. 793-824

Fig. 14

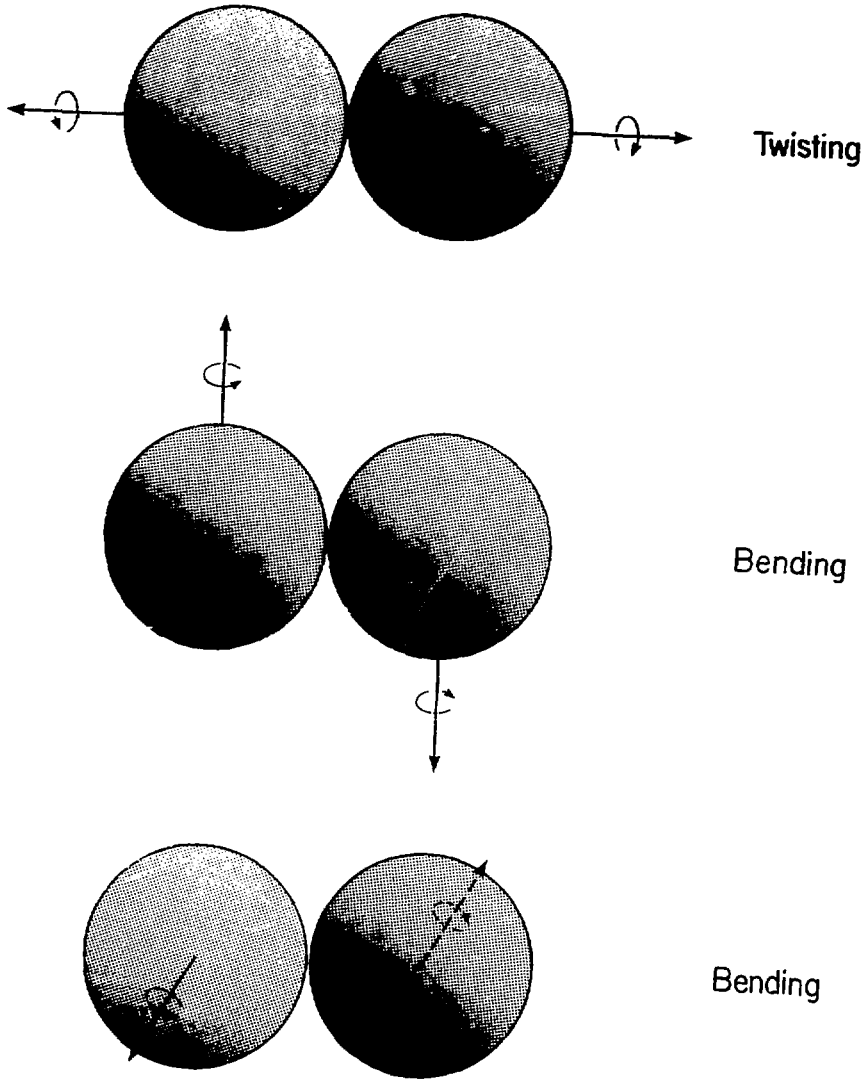

XBL 791-206

Fig. 1b

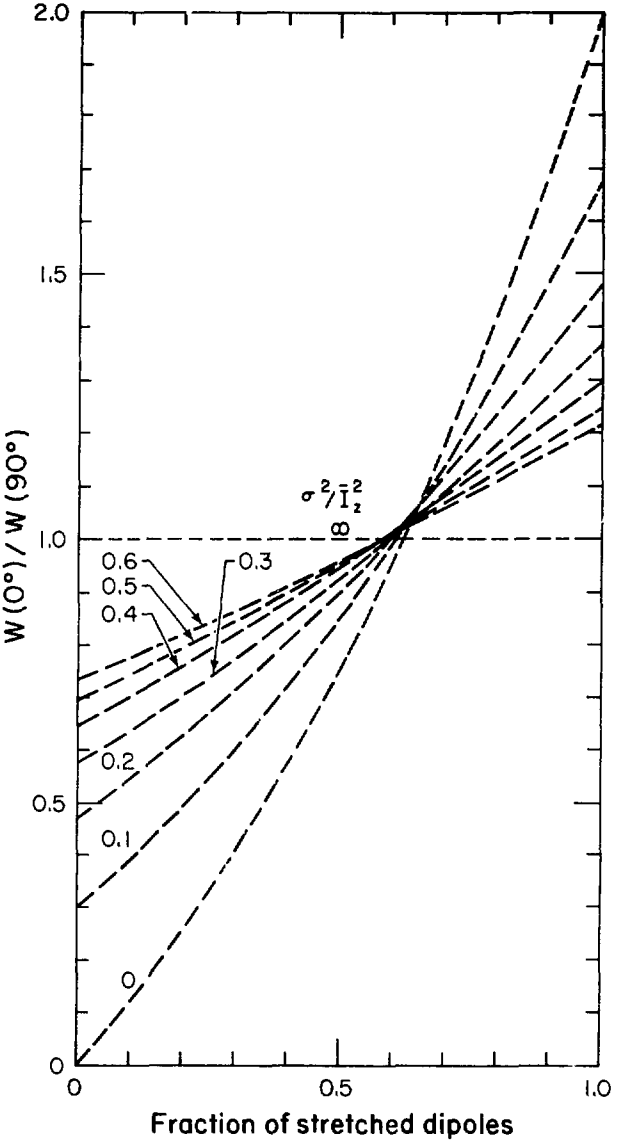

XBL 807-6999

Fig. 2a

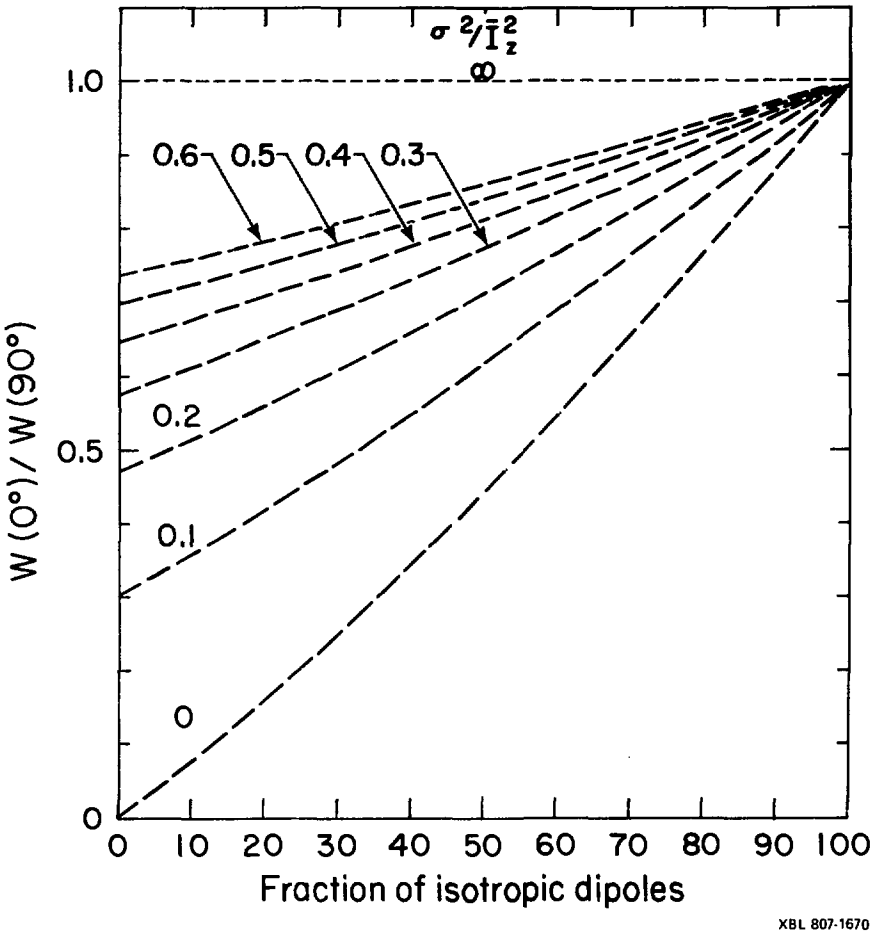
σ²/Ī²z
∞
0.6
0.5
0.4
0.3
0.2
0.1
0
1.0
0.5
0
W (0°) / W (90°)
0
10
20
30
40
50
60
70
80
90
100
Fraction of isotropic dipoles
XBL 807-1670

Fig. 2b

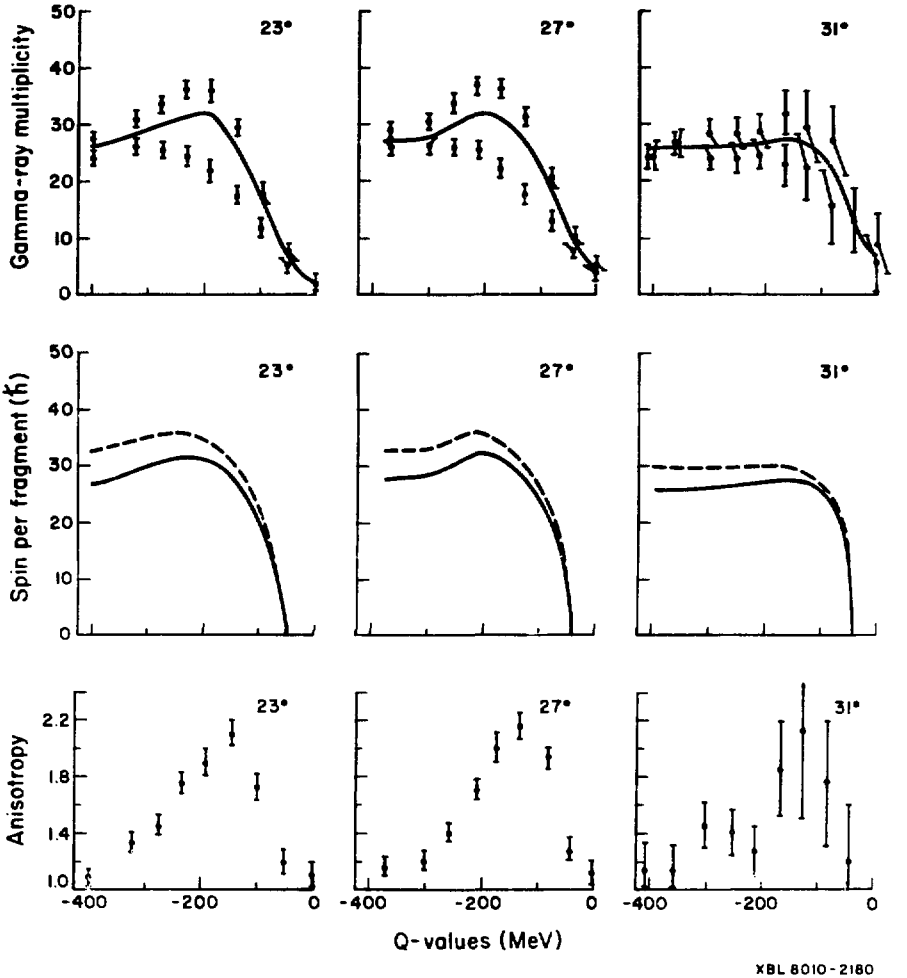
Gamma-ray multiplicity
Spin per fragment (ħ)
Anisotropy
23°
27°
31°
Q-values (MeV)
XBL 8010-2180

Fig. 3

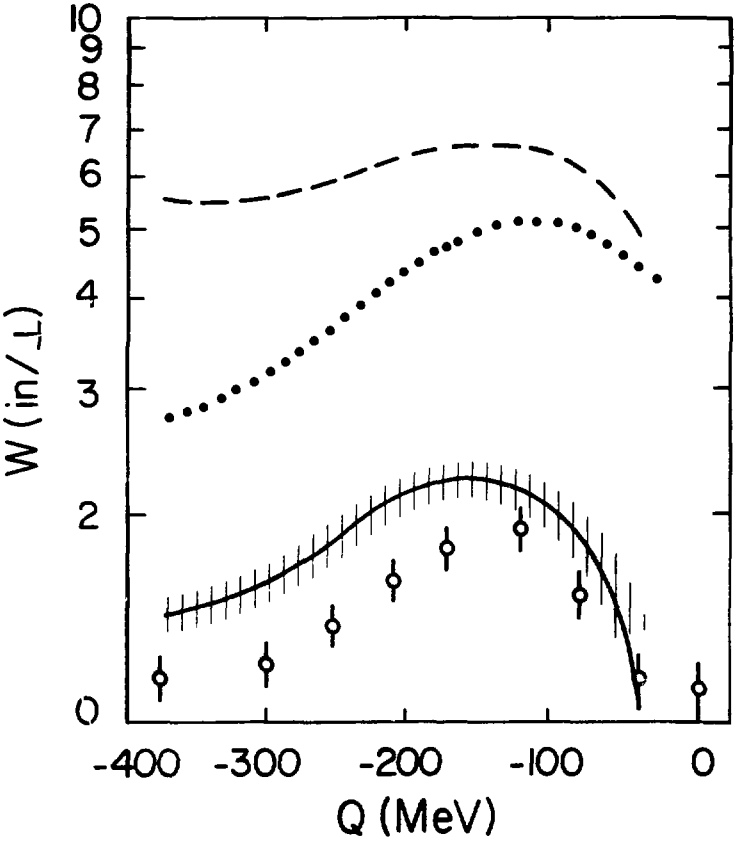

XBL 8012-2503

Fig. 4

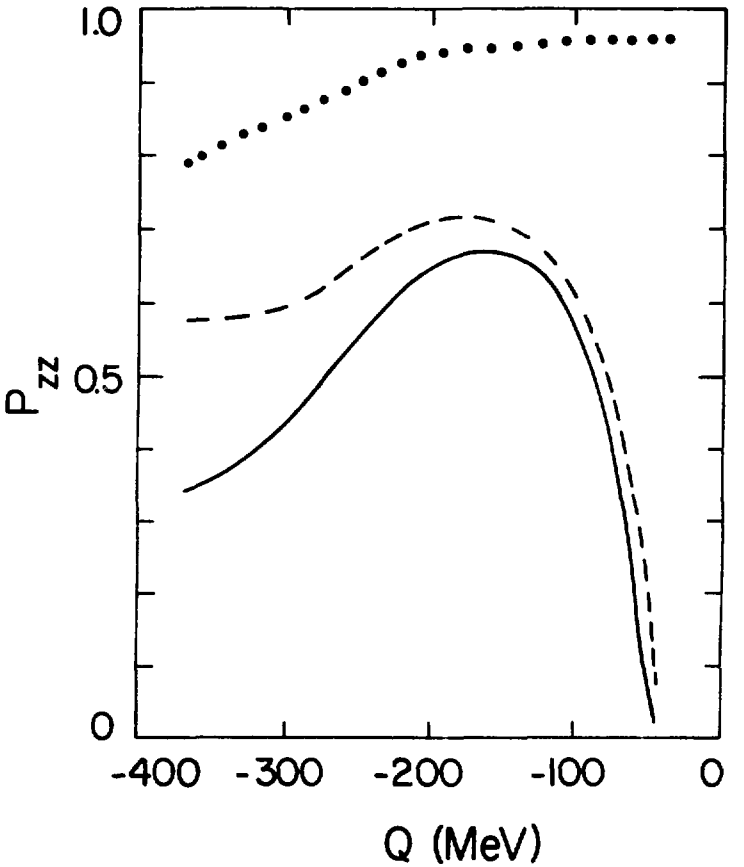

XBL 8010-2156

Fig. 5a

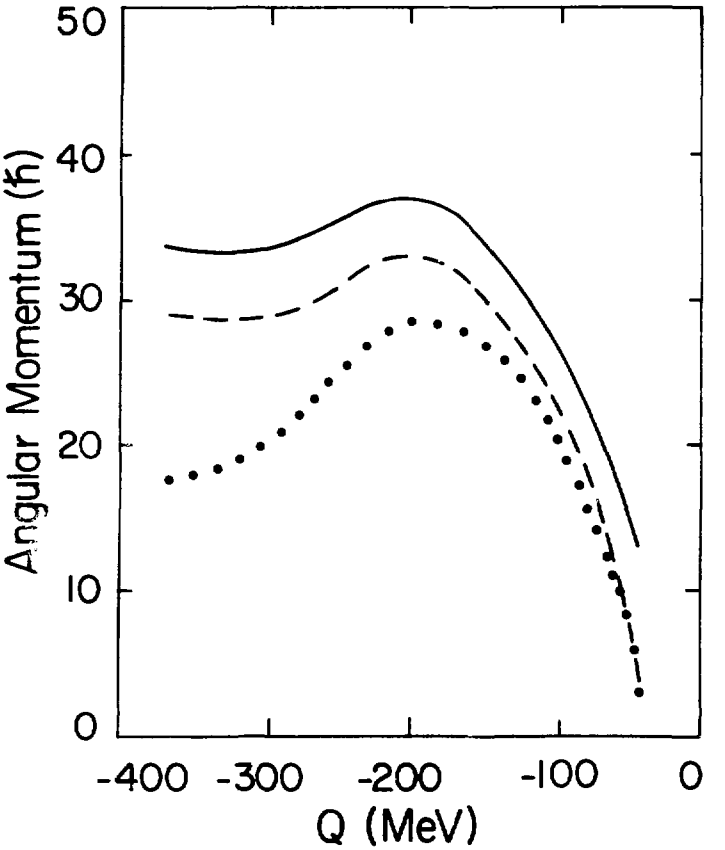

XBL 8010-2158

Fig. 5b

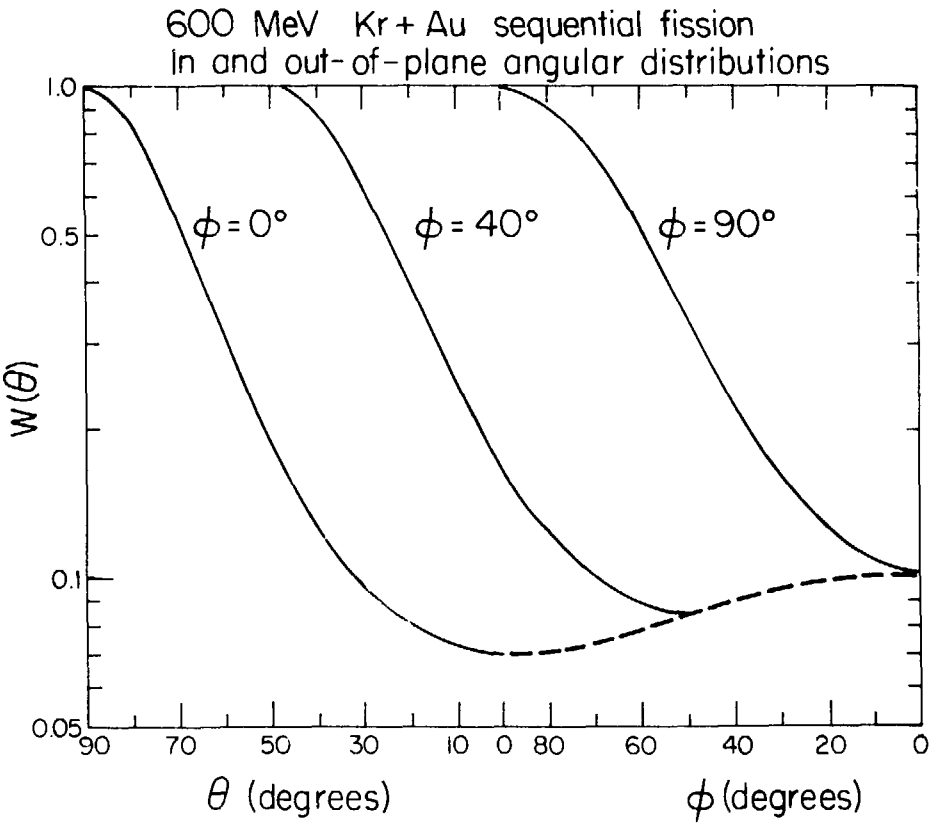

XBL 802-277

Fig. 6

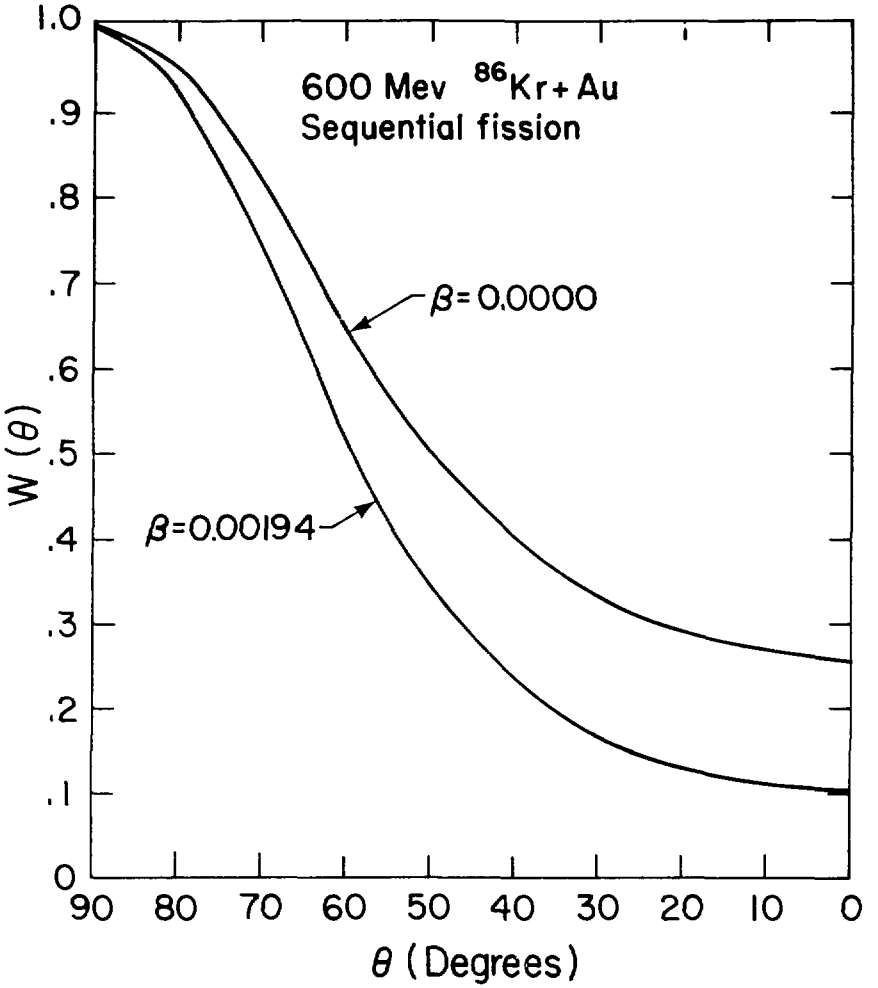

XBL 807-1672

Fig. 7

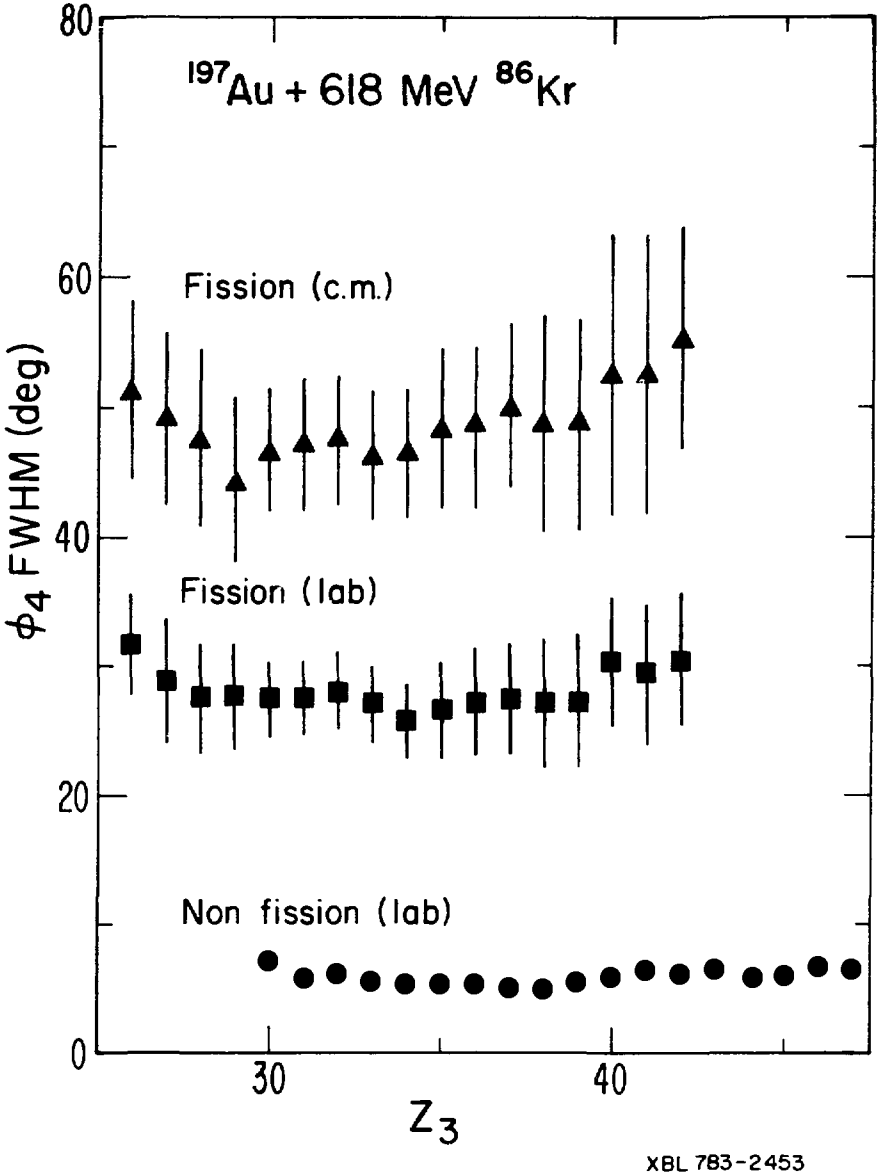
^{197}Au + 618 MeV ^{86}Kr
Fission (c.m.)
Fission (lab)
Non fission (lab)
ϕ_4 FWHM (deg)
Z_3
0
20
40
60
80
30
40
XBL 783-2453

Fig. 8

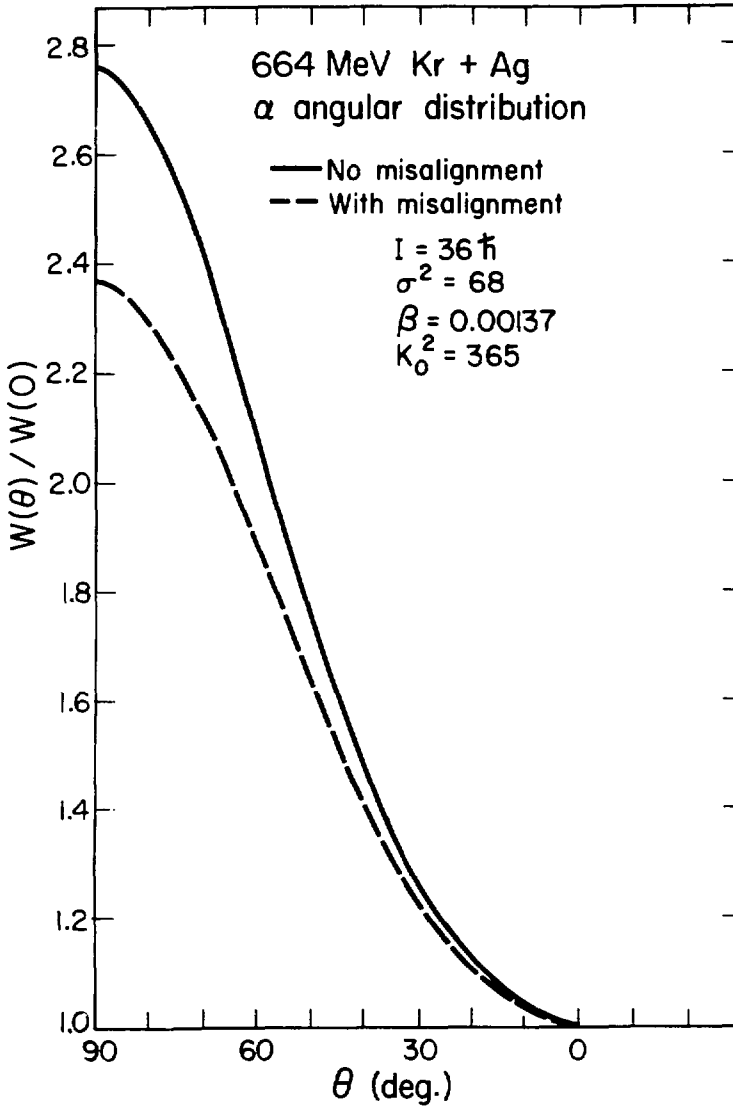

XBL 802-285

Fig. 9

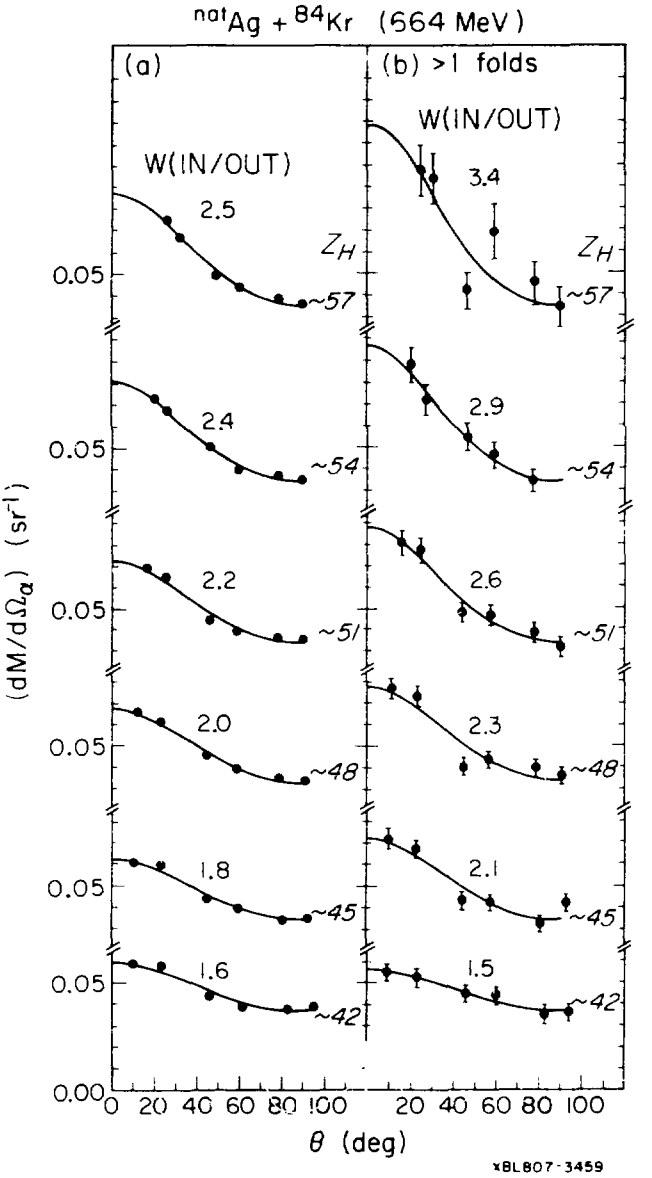
natAg + 84Kr (664 MeV)
(a)
(b) >1 folds
W(IN/OUT)
W(IN/OUT)
2.5
2.4
2.2
2.0
1.8
1.6
3.4
2.9
2.6
2.3
2.1
1.5
ZH
ZH
~57
~54
~51
~48
~45
~42
~57
~54
~51
~48
~45
~42
0.05
0.05
0.05
0.05
0.05
0.05
0.00
(dM/dΩα) (sr-1)
0 20 40 60 80 100
20 40 60 80 100
θ (deg)
xBL807-3459

Fig. 10

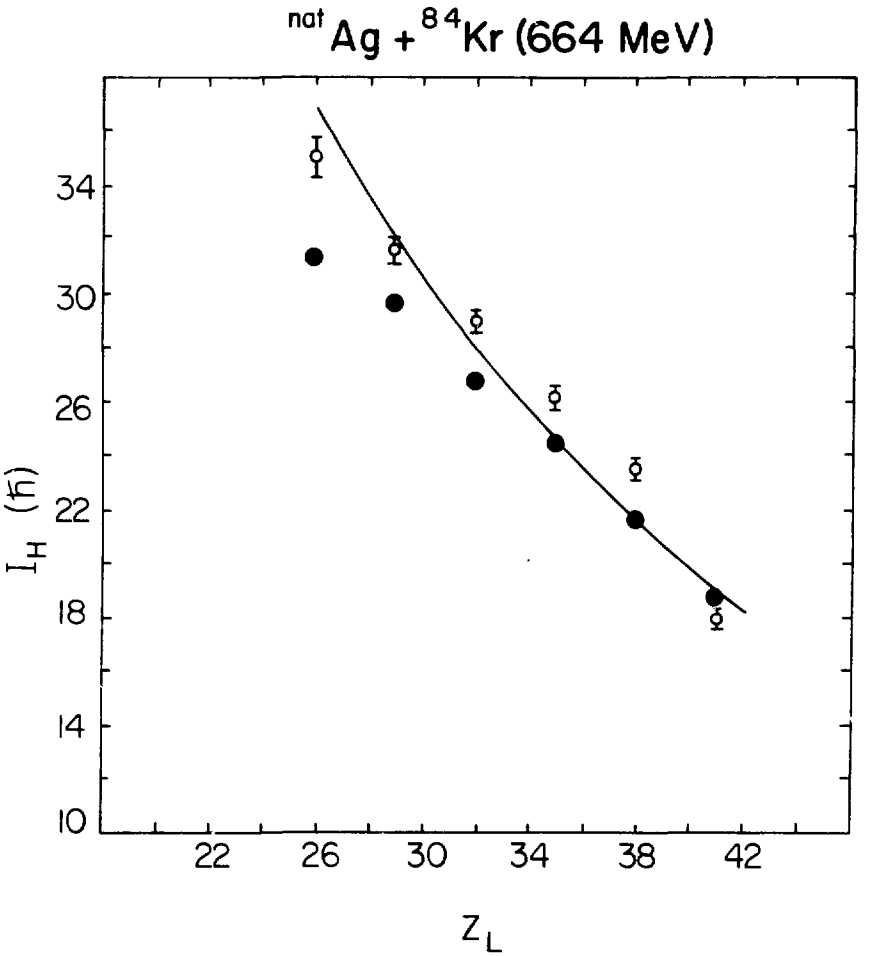

XBL 8010-2228

Fig. 11

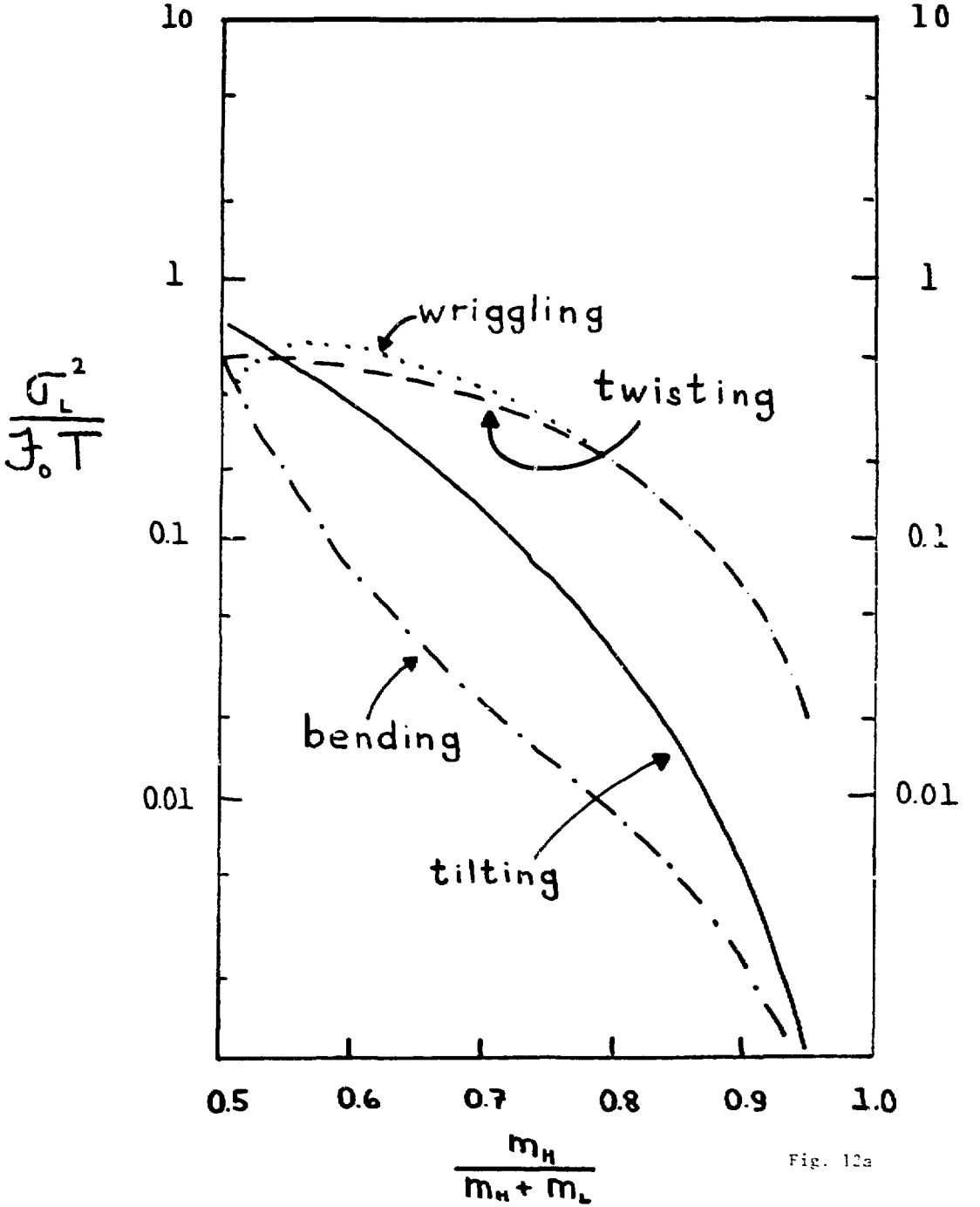
10
1
0.1
0.01
$\frac{\sigma_L^2}{\mathcal{F}_0 T}$
wriggling
twisting
bending
tilting
0.5
0.6
0.7
0.8
0.9
1.0
$\frac{m_H}{m_H + m_L}$

Fig. 12a

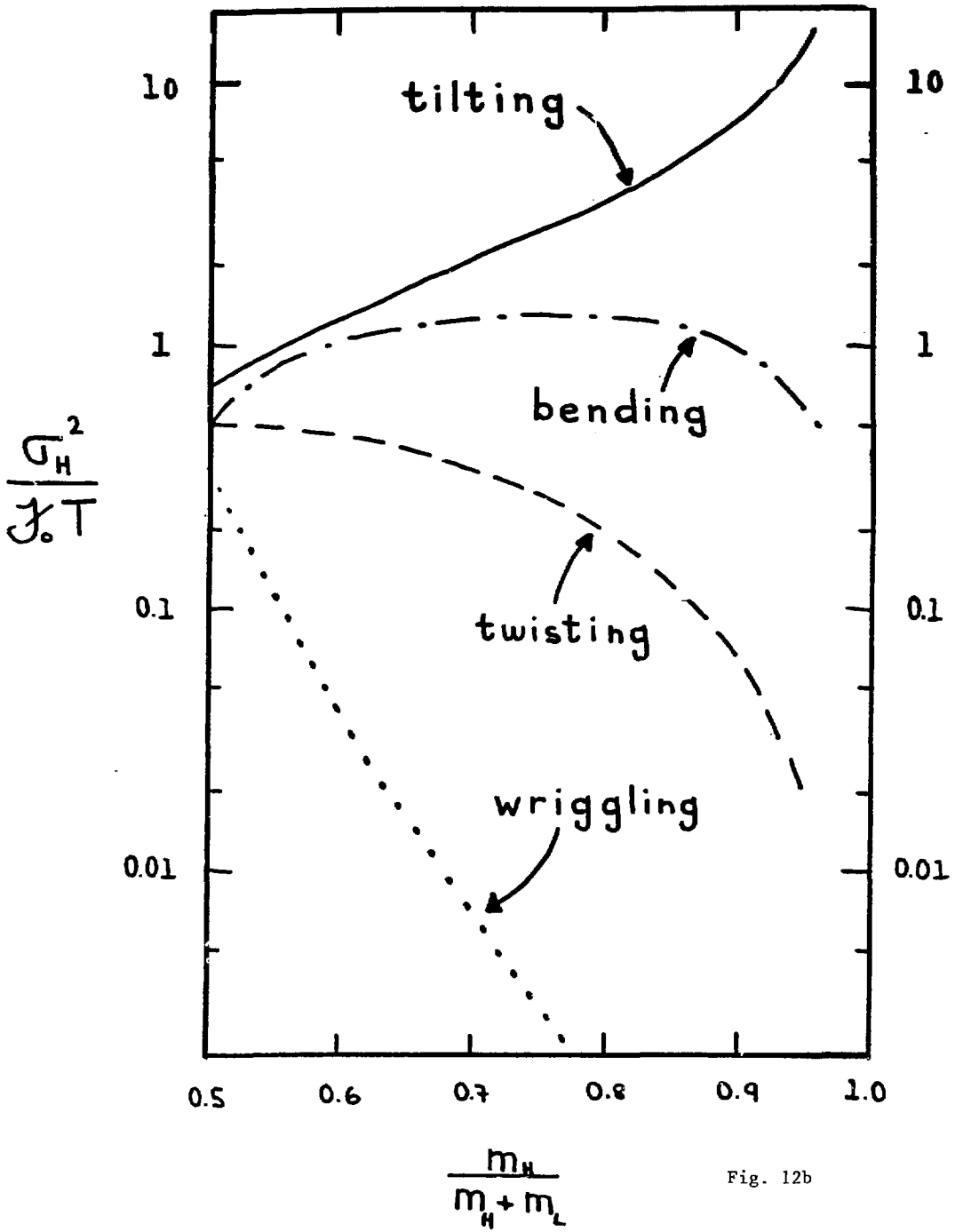
10
1
0.1
0.01
tilting
bending
twisting
wriggling
$\frac{\sigma_H^2}{\mathcal{J}_0 T}$
0.5
0.6
0.7
0.8
0.9
1.0
$\frac{m_H}{m_H + m_L}$

Fig. 12b

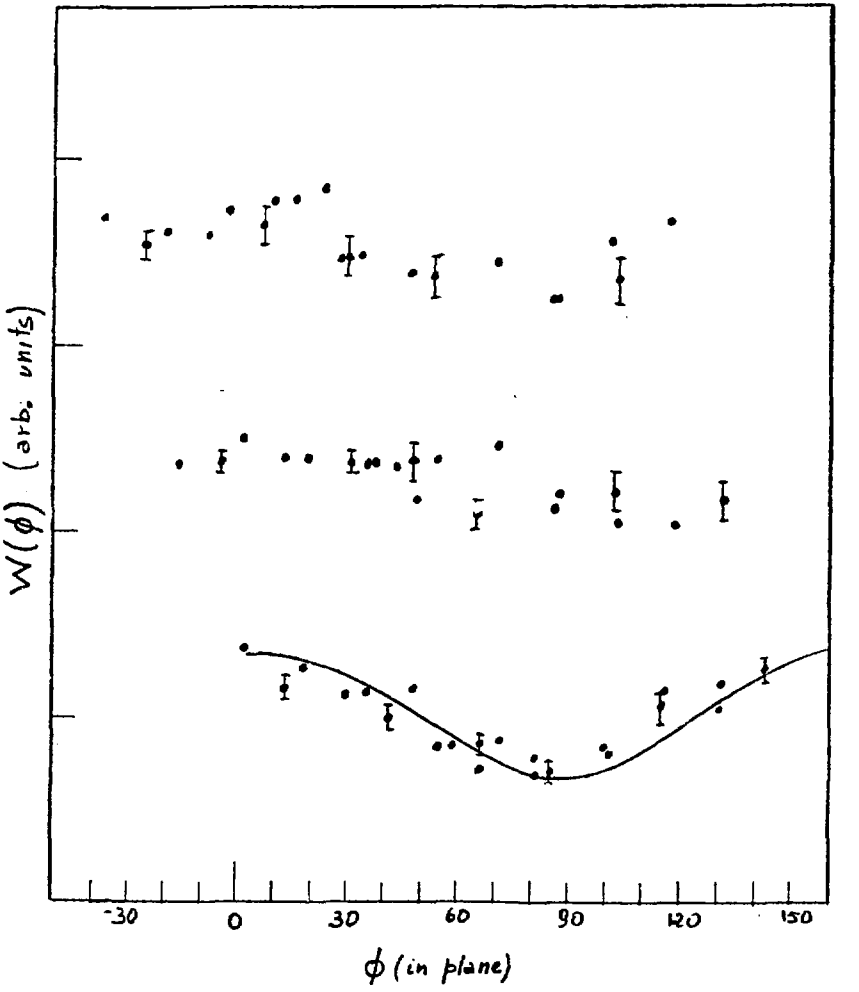

Fig. 13a

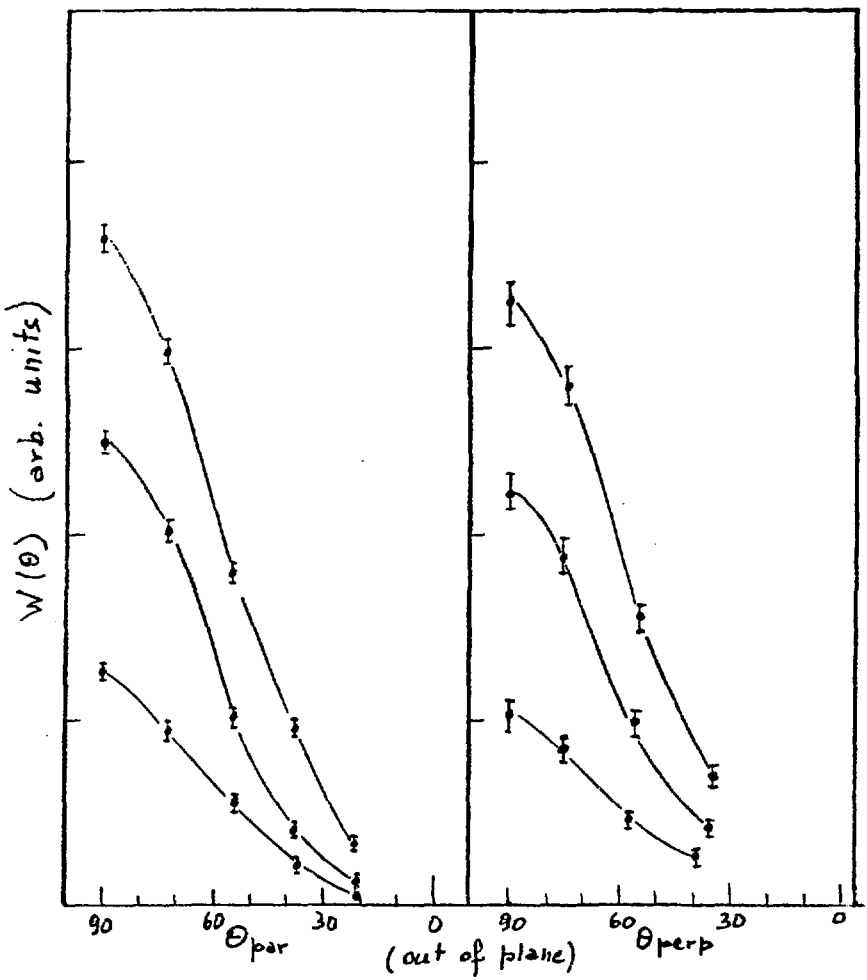

Fig. 13b